Comparison of Mechanical Behavior and Acoustic Emission Characteristics of Three Thermally-Damaged Rocks

Jun Peng [1,2,*] [ID] **and Sheng-Qi Yang** [2] [ID]

1   State Key Laboratory of Water Resources and Hydropower Engineering Science, Wuhan University, Wuhan 430072, China
2   State Key Laboratory for Geomechanics and Deep Underground Engineering, China University of Mining and Technology, Xuzhou 221008, China; yangsqi@hotmail.com
*   Correspondence: jun.peng@whu.edu.cn

Abstract: High temperature treatment has a significant influence on the mechanical behavior and the associated microcracking characteristic of rocks. A good understanding of the thermal damage effects on rock behavior is helpful for design and stability evaluation of engineering structures in the geothermal field. This paper studies the mechanical behavior and the acoustic emission (AE) characteristic of three typical rocks (i.e., sedimentary, metamorphic, and igneous), with an emphasis on how the difference in rock type (i.e., porosity and mineralogical composition) affects the rock behavior in response to thermal damage. Compression tests are carried out on rock specimens which are thermally damaged and AE monitoring is conducted during the compression tests. The mechanical properties including P-wave velocity, compressive strength, and Young's modulus for the three rocks are found to generally show a decreasing trend as the temperature applied to the rock increases. However, these mechanical properties for quartz sandstone first increase to a certain extent and then decrease as the treatment temperature increases, which is mainly attributed to the high porosity of quartz sandstone. The results obtained from stress–strain curve, failure mode, and AE characteristic also show that the failure of quartz-rich rock (i.e., quartz sandstone and granite) is more brittle when compared with that of calcite-rich rock (i.e., marble). However, the ductility is enhanced to some extent as the treatment temperature increases for all the three examined rocks. Due to high brittleness of quartz sandstone and granite, more AE activities can be detected during loading and the recorded AE activities mostly accumulate when the stress approaches the peak strength, which is quite different from the results of marble.

Keywords: thermal damage; compression test; mechanical behavior; acoustic emission; rock type

1. Introduction

With increasing energy demand, it is urgent in the present world to exploit new energy resources aside from fossil energy. Geothermal energy is a renewable and environment-friendly energy source which has gained much attention in recent years [1–4]. In order to exploit and use the geothermal energy efficiently, it is important to comprehensively investigate the mechanical characteristics and the associated thermal cracking mechanism of rocks under/after exposure to high temperature. A good understanding of high temperature effects on rock performance will help design and maintain long-term safety of engineering structures in geothermal energy systems.

The influence of high temperature on the physical and mechanical behavior of bedrocks in geothermal field has been systematically studied in recent years using laboratory testing methods.

It is found from the results from these laboratory studies that many physical and mechanical characteristics are largely affected by thermal damage. For example, the color of rocks after thermal treatment would generally become dark as a result of mineral transformations [5–7]. Li et al. [8] proposed to use colorimetry as a simple but effective method to assess fire damage of rocks. The hardness is found to generally weaken as the temperature applied to the rocks is gradually increased [9–12]. Similarly, with an increase in the applied temperature, the P-wave velocity showed a decreasing trend [13–15]. This was mainly associated with the microcracks generated by the thermal expansion of minerals [16,17]. As two important parameters in rock engineering design, the Young's modulus [18–22] and compressive strength [23–27] were also found to generally decrease as the treatment temperature increased. Some researchers also studied the tensile strength of rocks after thermal treatment and found that the tensile strength decreased with increasing temperature applied to rocks [28,29]. Nasseri et al. [30] conducted laboratory tests to examine the relation between fracture toughness and thermal damage. Their results revealed that the fracture toughness gradually decreased as the applied temperature was increased. On the other hand, the permeability were found to generally increase with increasing temperature in the treatment [31,32]. The relation between dynamic properties of rocks and thermal damage were also investigated by some researchers and it was found that the dynamic characteristics were also significantly influenced by thermal damage [33,34]. The investigated rocks in the above studies included granite, marble, sandstone, limestone, gabbro, claystone, calcarenite, etc. However, due to the differences in mineralogical composition, grain size distribution, degree of weathering, and microstructures, the obtained physical and mechanical responses for various rock types were different.

Many microscopic observation techniques have been used in recent years to elucidate the microcracking mechanism associated with thermal damage. These techniques include acoustic emission (AE) [35–37] and scanning electron microscopy (SEM) [38–40]. The results from these microscopic observation techniques showed that the decrease of rock macroproperties with the increase of thermal damage is to a large extent attributed to the development of microcracks inside the rock specimen [41–43]. In general, two kinds of thermally-induced microcracks can be found in rock due to the applied thermal stress which are usually named as thermal gradient microcrack and thermal cycling microcrack [44]. The thermal gradient microcracks are mainly associated with the inhomogeneous strain field which is generated by the non-uniform temperature applied to the rock. The thermal cycling microcracks are related to the mismatch between the thermal expansion coefficients of the different minerals constituting the rock. Under low temperature conditions, most of the thermally-generated microcracks were along the grain boundaries. As the applied temperature increased, the intra-granular cracking were found to be intensive and the generated intragranular microcracks had a large effect on the rock macroproperties [45–47]. For crystalline rocks, the thermally-generated cracks were found to mainly develop at the boundaries of quartz [48]. This is mainly due to the fact that the thermal expansion coefficient of quartz is obviously larger than that of other minerals [49]. To better understand the influence of high temperature on the physical and mechanical property and more importantly the associated microcracking mechanism, this study experimentally investigates the mechanical behavior and the AE characteristic of three typical rocks forming under different geological environments (i.e., quartz sandstone, marble, and granite). Compression tests are carried out on rock specimens which are exposed to different high temperatures. During the compression tests, the AE technique is applied to monitor the AE signals in the entire loading process. The influences of thermal damage on the mechanical property and the AE characteristic of the three rocks are then compared and examined. Since the mineral composition and texture of the three rocks are different, the main focus of this study is elucidate how the difference in the rock type affects the mechanical behavior and the AE characteristics.

2. Materials and Methodology

2.1. Description of Rock Specimen

The rocks studied in this paper are quartz sandstone, marble, and granite. The quartz sandstone was collected from the reservoir region of the Three Gorges project, Zigui City, China. A rock block with the dimension of 400 mm in length, 300 mm in width, and 200 mm in height was collected and shipped to Wuhan University, China for specimen preparation and testing. The marble was collected from a copper mine in Zhenping City, China and a massive rock block with the dimension of 600 mm in length, 500 mm in width, and 150 mm in height was collected. The physical and mechanical properties of the marble with different degrees of thermal damage were previously investigated by Rong et al. [17] and the results of the marble are discussed in this paper for comparison. The granite was collected from a mine in Suizhou City, China. The collected rock block has a length of 280 mm, a width of 200 mm, and a height of 200 mm.

The Zigui quartz sandstone has a clastic texture. It is relatively isotropic and no visible fractures could be found in the rock sample. The grain size ranges from 0.1 mm to 0.5 mm, which is classified as fine-to-medium grained. The rock is mainly composed of quartz, feldspar, mica, calcite, and clay. The Zhenping marble has a crystalloblastic texture. It is mainly composed of calcite (i.e., approximately 95 percent of the whole volume). The grain size is in the range of 1.5 to 2.5 mm and its mean value is about 2 mm. The rock is classified as coarse-grained. The texture is found to be generally isotropic and there is no obvious foliation. The Suizhou granite is a plutonic acid igneous rock, which has a porphyritic texture. The rock is mainly composed of quartz and feldspar, with small amount of mica, hornblende, and pyroxene. The grain size ranges from 2.0 mm to 4.0 mm.

The examined Zigui quartz sandstone is a sedimentary rock, which is formed in the process of deposition and subsequent cementation. Based on the mineralogical composition, the rock is probably generated from quartz-rich igneous rocks such as granite. There is no preferred layer plane in the rock, indicating that the deposition behavior is generally homogenous and isotropic. The Zhenping marble is a typical metamorphic rock and it is formed in the process of metamorphism. Because the color of the marble is pure white with some milk gloss, it is indicated that it is generally formed at a low-to-medium temperature condition. The collected marble is generally massive and the degree of crystallinity is high. The Suizhou granite is a typical igneous rock, which is formed in the process of magmatism. Because the granite is dark in color, it is indicated that the rock may form at a deep ground in earth. In general, both of quartz sandstone and granite investigated in this study are mainly composed of quartz, it is inferred that the two rocks will be more brittle than marble.

To ensure the properties of the examined rock specimens are generally the same for each rock type, all rock specimens of each rock type are drilled out from the same rock block. The drilling is along the short dimension of the rock block and the inner diameter of the coring bit is about 50 mm. All specimens are cut to have a length of 100 mm and the height-to-diameter is approximately 2. Ends of the prepared specimens are then ground to be smooth [50]. Figure 1 shows the prepared specimens for the three typical rocks. All prepared rock specimens are air-dried and maintained in a chamber for the following thermal treatment and laboratory tests.
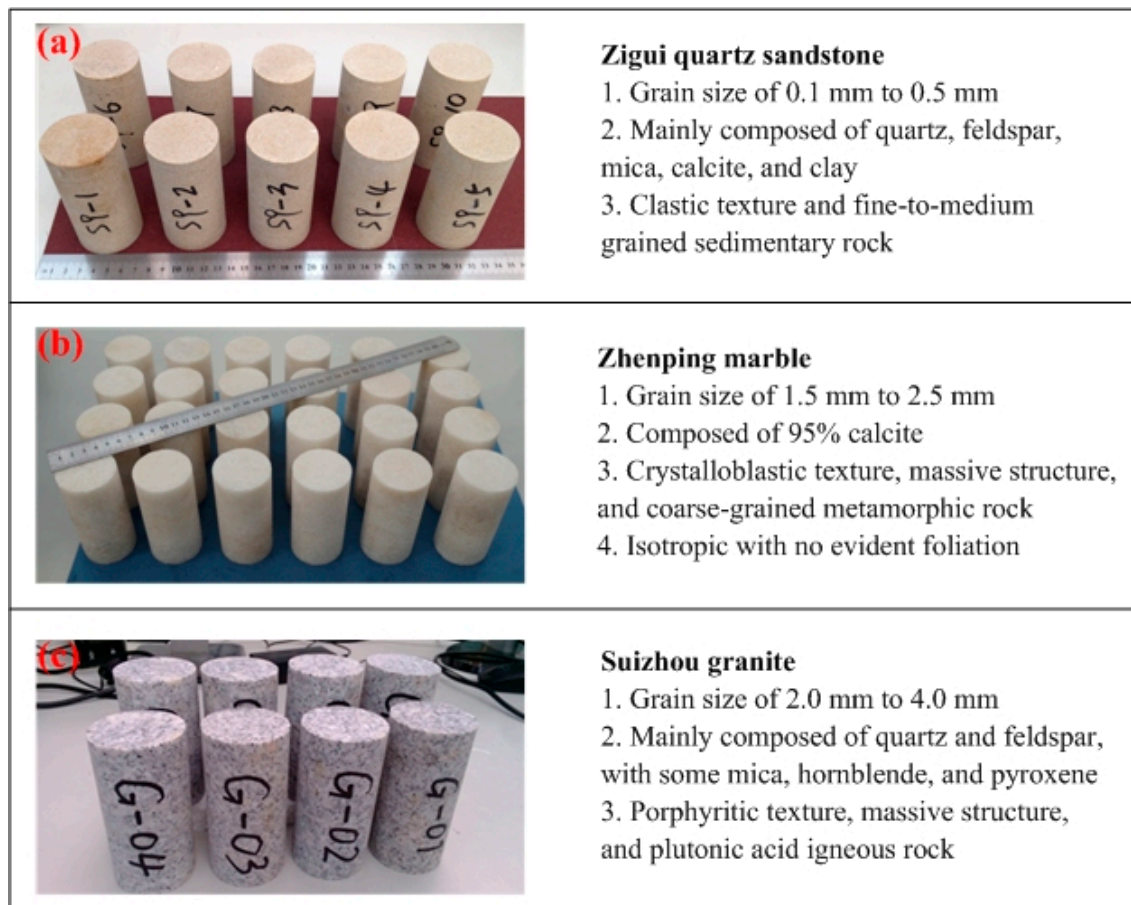
Figure 1. Prepared specimens of three typical rocks for laboratory tests.

The physical properties of the three typical rocks are measured before laboratory testing. Table 1 summarizes the measured physical properties. These physical parameters are determined using the methods recommended by ISRM [50]. It is found that the quartz sandstone has the largest porosity and the corresponding P-wave velocity is much lower when compared with that of the other rocks.

Table 1. Physical properties of the specimens of three typical rocks before thermal treatment.

| Rock Type	Bulk Density (g/cm^3)	Grain Density (g/cm^3)	Saturation Density (g/cm^3)	Total Porosity (%)	Effective Porosity (%)	P-Wave Velocity (km/s)
Quartz Sandstone	2.402	2.672	2.463	10.10	6.11	4.786
Marble	2.699	2.720	2.702	0.77	0.30	5.814
Granite	2.823	2.861	2.831	1.33	0.80	5.430

2.2. Experimental Procedure

In this study heating was applied using a resistance furnace. As shown in Figure 2a, the heating device is composed of a control cabinet and a container. The maximum temperature for the furnace is 1200 °C and the rated power is about 10 kW. The thermal treating procedure is presented in Figure 2b. Firstly, the specimens are heated in the furnace to a predetermined temperature with a heating rate of 10 °C/min. Once the predetermined temperature is reached, all specimens are still kept in the furnace for about 4h. Afterwards, the specimens are taken out of the furnace till the room temperature is reached. Several groups of temperatures are examined in this study for different rock types. The temperatures investigated for the quartz sandstone are 25 °C (room temperature),

200 °C, 400 °C, 600 °C, 800 °C, and 1000 °C. The examined temperatures for the marble are 25 °C, 200 °C, 400 °C, and 600 °C. The temperatures for the granite are 25 °C, 400 °C, 600 °C, and 800 °C. The maximum predetermined temperature for marble is lower when compared that of the other two rocks. This is because if a marble specimen is heated to a higher temperature (i.e., 800 °C), the specimen can be easily destroyed with bare hand.
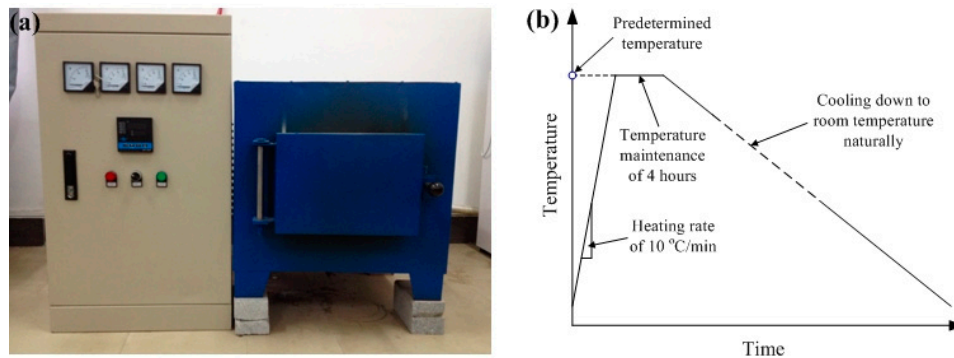
Figure 2. Heating device and procedure for thermal treatment. (**a**) A box-type resistance furnace; and (**b**) Thermal treating procedure used in this study.

The compression tests in this study were performed using a hydraulic servo-controlled test system, which consists of a pressure chamber, a loading frame, and the measurement and control electronics (see Figure 3a). The maximum confining pressure for the testing machine is about 100 MPa, with the maximum load capacity of 300 kN. The ranges of measurement for axial and lateral displacement transducers are 8 and 4 mm, respectively. Before compression tests, both displacement transducers are carefully calibrated. In the present study, the quartz sandstone and marble specimens are tested under uniaxial loading and the granite specimens are tested under triaxial loading with a confining pressure of 10 MPa. Under uniaxial loading, an axial displacement-controlled loading is applied to the rock specimens with a loading rate of 0.075 mm/min. Under triaxial loading, the confining pressure is first applied using a loading rate of 0.25 MPa/s and the specimens are then loaded to failure with a loading rate of 0.075 mm/min.
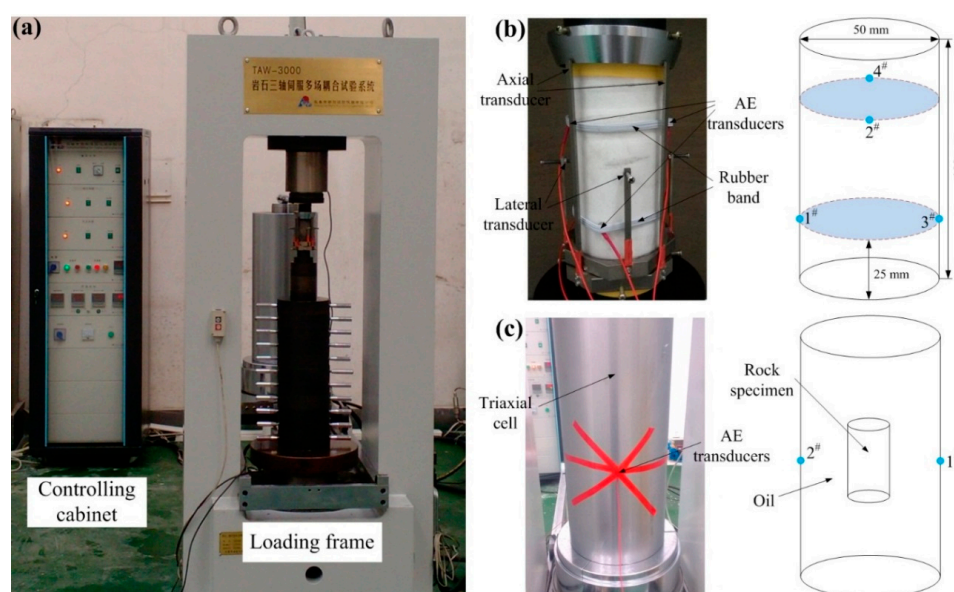
Figure 3. Machine for compression tests with AE monitoring. (**a**) Overview of the compression system; (**b**) AE setup for uniaxial compression tests; and (**c**) AE setup for triaxial compression tests.

During the compression tests, AE detection model PCI-2 is used to monitor the AE signals and the used AE transducers are piezoceramic-type. The resonance frequency of the AE transducers ranges from 100 to 400 kHz. A detection threshold is set to be 50 dB and the gain value for pre-amplifier is set to be 40 dB. This is to ensure an effective detection of AE signals while minimizing the influence of background noise on the recorded AE results.

In uniaxial compression tests, four AE transducers are used and directly mounted onto the surface of the specimen. As shown in Figure 3b, two AE transducers are detached in the upper part of the specimen and the other two are detached in the lower part of the specimen. The height of the AE transducers is about 1/4 of the height in the specimen (i.e., 25 mm). An orthogonal layout can ensure a good coverage of the whole specimen. In addition, a layer of white Vaseline is used between the contact of the AE transducer and the specimen surface, which can ensure a good acoustic coupling. In order to fix the transducers, two loops of rubber band is used. The width of the rubber band is basically the same as the diameter of the AE transducer. Prior to testing, pencil lead fracture tests are conducted to check the coupling between specimen surface and AE transducers. In the pencil lead fracture test, a minimum amplitude of 95 dB is guaranteed, which indicates an effective coupling. In triaxial compression tests, because the used AE transducer cannot sustain high pressure in the triaxial cell, two AE transducers are symmetrically installed in the front and back of the triaxial cell surface, with a height equal to the center of the specimen (see Figure 3c).

3. Results and Discussion

3.1. Mechanical Behavior

3.1.1. P-Wave Velocity

Wave velocity is a parameter which is sensitive to the microcracks residing inside the rock specimen. This parameter is generally used to quantitatively assess the thermally-induced microcrack damage. In this study, P-wave velocities of rock specimens of different types after exposure to different treatment temperatures are measured using an ultrasonic pulse transmission technique. The P-wave velocity is measured along the long axis of the specimen. Two transducers are fixed in the center of each end of the specimen. Similarly to the AE monitoring, Vaseline is used in the contact of the transducers and the specimen. This is to ensure that the energy can be effectively transferred between the transducers and the specimen. In the P-wave velocity measurements, a frequency of 1 MHz is used for the waves. In addition, the transducers are calibrated prior to the tests. To have a reliable results, P-wave velocity is tested five times for each specimen.

Variations of P-wave velocities of different rocks with treatment temperatures are presented in Figure 4. It is seen that P-wave velocities of the three rocks are significantly affected by the thermal treatment. As the temperature in the treatment gradually increases, the P-wave velocities generally present a decreasing trend. For marble and granite specimens, the P-wave velocities show a monotonous decrease as the treatment temperature increases. The P-wave velocity decreases by 87.0% and 80.1% respectively for marble and granite at the maximum treatment temperature when compared with those for specimens without thermal treatment. For quartz sandstone, the P-wave velocity first increases to some extent under low treatment temperature and then decreases dramatically as the applied temperature increases.
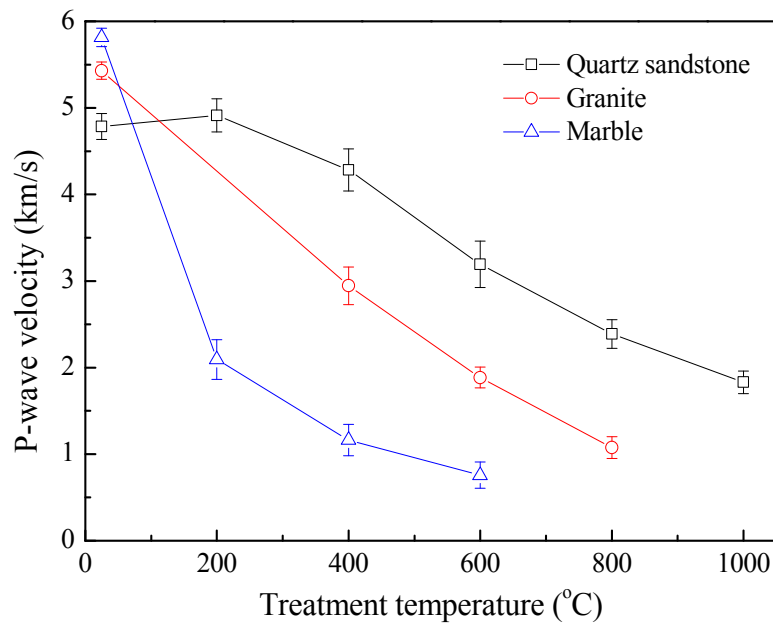
Figure 4. Variation of P-wave velocity of the examined rocks with treatment temperature.

The difference of P-wave velocity variation in response to the change of treatment temperature is mainly associated with the difference in microstructure of the rock specimens. Because the examined quartz sandstone has a large porosity when compared with that of marble and granite, the thermal treatment with low temperature may result in a local crack closure inside the rock specimen, which may lead to a slight increase in the P-wave velocity. In addition, water in the pores of the specimen will evaporate when the thermal stress is applied, which may also result in an increase of the measured P-wave velocity. On the contrary, the marble and granite have a low porosity and the mineral grains in these two specimens are found to be well cemented. Hence, the deformation space is generally small for the mineral expansion inside the specimen. Microcracking will occur inside the rock even when the treatment temperature is low. This is why the P-wave velocity of marble and granite shows a monotonous decrease in response to the change of the treatment temperature.

3.1.2. Strength and Modulus

The variations of peak strength in response to the change of the treatment temperature are presented in Figure 5a. It is seen that the thermal treatment generally weakens the peak strength of different rocks. For marble and granite, a monotonous decrease of peak strength with increasing treatment temperature can be observed, which is similar to the results of the P-wave velocity. The peak strength decreases by 44.4% and 33.3%, respectively, for marble and granite at the maximum treatment temperature when compared with those for specimens without thermal treatment. On the other hand, the peak strength for quartz sandstone is found to increase first with low temperature (i.e., lower than 200 °C) in the treatment and decreases dramatically with an increase in the treatment temperature. The phenomenon is also mainly associated with the formation and microstructure of the examined rocks. A temporary crack closure may occur at quartz sandstone when it is thermally treated with low temperature due to its high porosity. The results reveal that the rock strength behavior is also very sensitive to the porosity of the examined rock. It should be noted that because the granite specimens are loaded under a confining pressure of 10 MPa, the peak strength of granite is much higher when compared with those of marble and quartz sandstone.
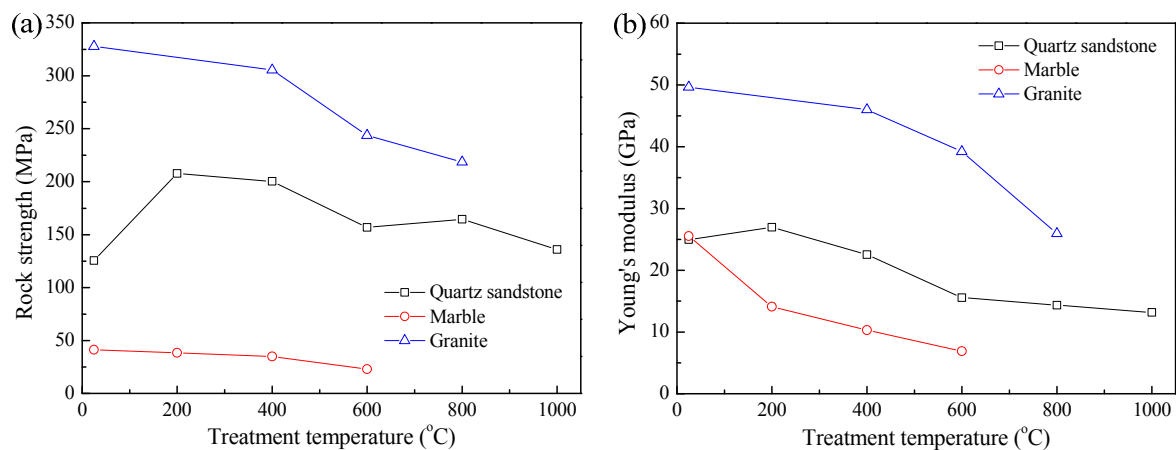
Figure 5. Variation of (**a**) rock strength and (**b**) Young's modulus of the examined rocks in this study with treatment temperature.

Figure 5b presents the variations of Young's module of different rock types with the treatment temperature. The Young's modulus in this study refers to the tangent modulus. The linear segment in the stress–strain curve is used to determine the Young's modulus. The results show that the thermal treatment has a large influence on the Young's modulus of the examined rocks. Because the granite specimens are loaded under a confining pressure of 10 MPa, the Young's modulus of granite is found to be much higher than those of marble and quartz sandstone. The Young's module of different rocks are generally weakened as the treatment temperature gradually increases. However, like the peak strength results, the weakening behavior of Young's modulus for different rock types is slightly different. The Young's module of marble and granite monotonously decrease with an increase in the treatment temperature. The Young's modulus decreases by 73.0% and 47.8%, respectively, for marble and granite at the maximum treatment temperature when compared with those for specimens without thermal treatment. On the other hand, the Young's modulus for quartz sandstone first increases with low temperature in the treatment and then decreases dramatically with an increase in the treatment temperature, which is associated with the temporary crack closure resulted from its high porosity.

3.1.3. Stress–Strain Relation

The stress–strain relations of different rocks after treatment with different temperatures are also compared and examined. Figure 6 presents the complete stress–strain relations of quartz sandstone under different treatment temperatures. The results show that the thermal treatment significantly affects the stress–strain relations. When the treatment temperature is lower than 400 °C, the initial deformation stage is found to be elastic linear (see Figure 6a). However, when the treatment temperature is higher than 600 °C, the nonlinearity in the initial deformation stage of the stress–strain curve is greatly increased. The increase in nonlinearity of the initial deformation stage is an indicator to characterize the thermally-induced microcrack damage inside the rock specimen [51]. The results indicate that many microcracks have been generated inside the rock specimen when the treatment temperature is higher than 600 °C, which is mainly associated with the phase transformation of quartz mineral. The maximum volumetric deformation during loading of quartz sandstone is found to generally increase as the treatment temperature increases (see Figure 6b). Because more microcracks are generated inside the rock specimen with an increase in the treatment temperature, the compression capacity is more prominent in specimens after thermal treatment with a higher temperature, leading to a larger volumetric deformation under compression.
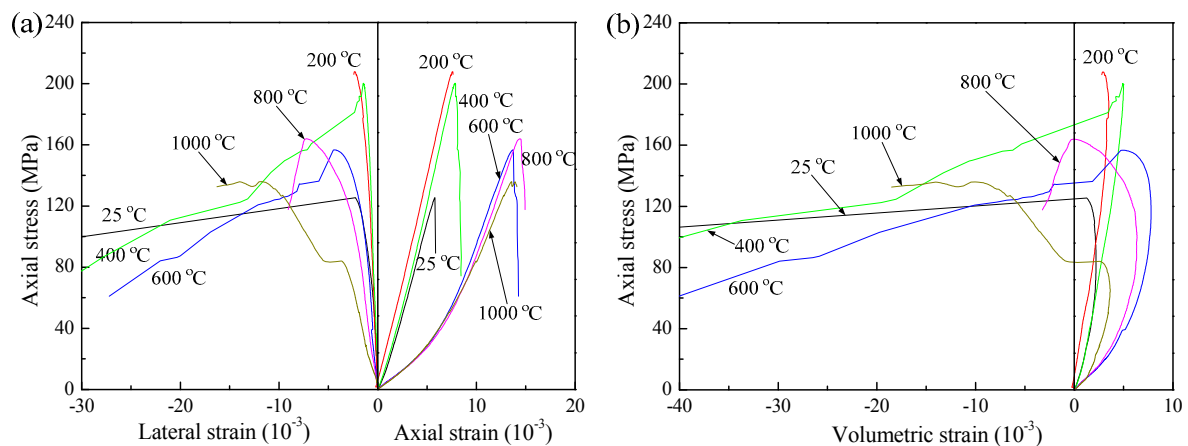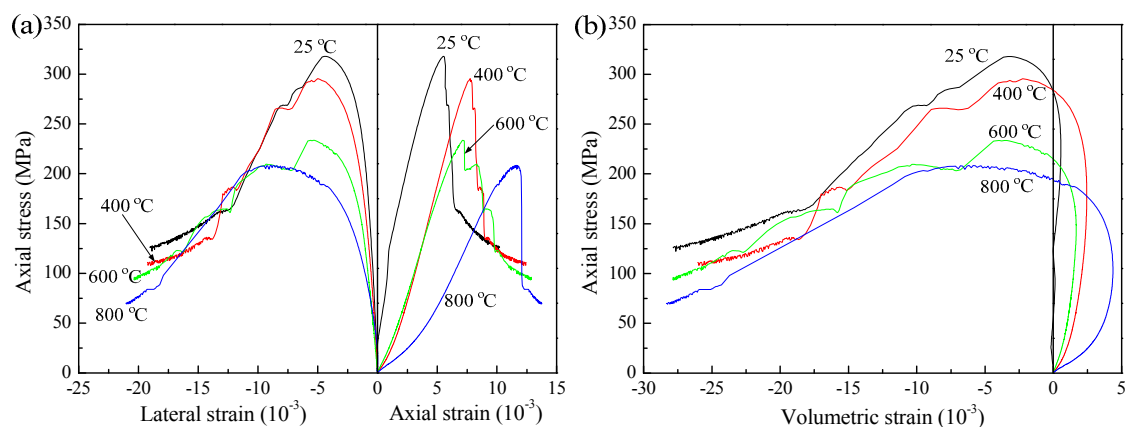
Figure 6. Stress–strain relations of quartz sandstone specimens in terms of (**a**) axial and lateral strains and (**b**) volumetric strain.

The stress–strain relations of marble under different treatment temperatures are reported by Rong et al. [17] and the readers can refer to that publication for the results. A gradual increase can be observed for the nonlinearity in the initial deformation stage of the stress–strain curve when the temperature in the treatment increases. The results reveal that the thermally-induced microcracks become more prominent with the increase in the treatment temperature. It is also seen that the maximum volumetric deformation of marble specimen generally increase as the treatment temperature increases.

Figure 7 shows the stress–strain relations of granite under different treatment temperatures. Similarly to the results of quartz sandstone and marble, the nonlinearity in the initial deformation stage of the stress–strain curve is found to gradually increase as the treatment temperature increases. The nonlinearity in the initial deformation stage of specimen after treatment with 800 °C is much more prominent when compared with that of specimen after treatment with lower temperature. The results also show that the maximum volumetric deformation of granite specimen generally increases with the increase in the treatment temperature.


Figure 7. Stress–strain relations of granite specimens in terms of (**a**) axial and lateral strains and (**b**) volumetric strain.

By comparison of the stress–strain relations of the three rocks, it is seen that the rock generally fails in a brittle manner, i.e., the stress drops to a low level rapidly in the post-peak deformation stage. However, with an increase in the treatment, the stress–strain curve for marble specimen changes from brittle to slightly strain-softening [17]. The results show that the ductility of marble is slightly increased

as the treatment temperature increases. It is also seen from the results that the quartz sandstone and granite are more brittle than the marble. The results are in a good agreement with those obtained from geological characteristic of the examined rocks. In addition, the increase in the nonlinearity of the initial deformation stage with increasing treatment temperature for marble is more stable and smooth when compared with those of quartz sandstone and granite. The nonlinearity in the initial deformation stage of the stress–strain curve is only prominent when the applied temperature is above 600 °C. This is mainly due to the fact that the α-β transition of quartz is about 573 °C.
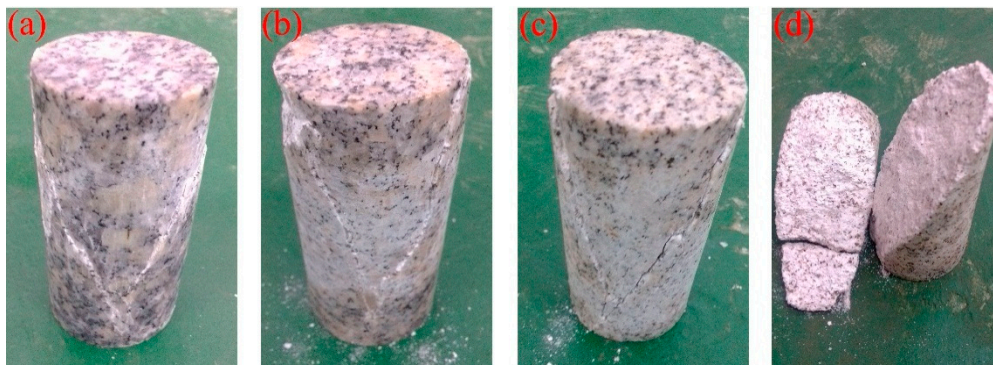
3.1.4. Failure Mode

Figure 8 presents the failure modes of the quartz sandstone specimens with different temperatures in the treatment. It is seen from the results that the failure mode of the rock is significantly affected by the thermal treatment. All the tested quartz sandstone specimens generally fail in a brittle splitting manner. However, the integrity after failure is different for rock specimens with different temperatures in the treatment. For rock specimens under higher treatment temperature, the integrity is generally lower when compared with those under lower treatment temperature. More fragments can be observed after the failure of the specimen as the treatment temperature gradually increases. The degradation of specimen integrity after failure can be used as an indication to assess the thermal damage [16,34].
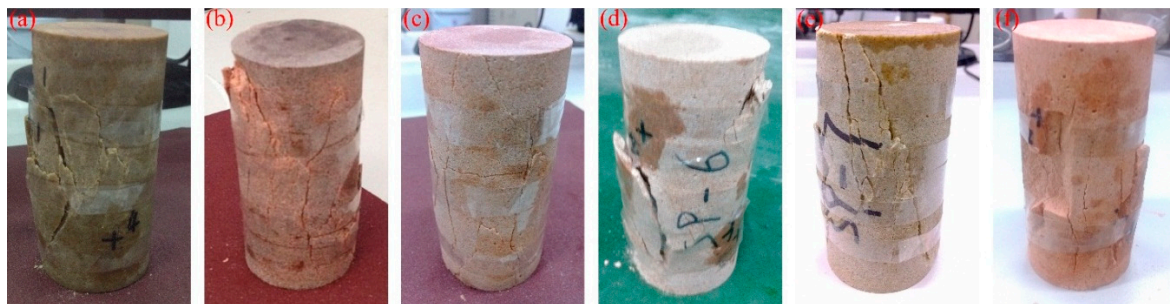
Figure 8. Failure modes of quartz sandstone specimens under different treatment temperatures. (**a**) 25 °C (room temperature); (**b**) 200 °C; (**c**) 400 °C; (**d**) 600 °C; (**e**) 800 °C; and (**f**) 1000 °C.

The failure modes of marble specimens under different treatment temperatures were reported by Rong et al. [17]. It is seen from the results that the failure mode of the rock is significantly influenced by the thermal treatment. The specimen with low temperature in the treatment fails in a brittle splitting manner. However, the failure changes from splitting to single shear as the treatment temperature increases. The results reveal that the ductility of marble specimen is greatly enhanced due to thermal treatment, which is in a general good agreement with the results obtained from the stress–strain relation. Similarly to the results of quartz sandstone, more fragments can be observed after the failure of the specimen with an increase in the treatment temperature.

The failure modes of the granite specimens with different temperatures in the treatment are presented in Figure 9. Failure mode of the granite specimen is significantly affected by the thermal treatment. In general, because the granite specimens are loaded under a confining pressure of 10 MPa, the failure of all the tested granite specimens is shear. However, the integrity of the granite specimen after failure is different. When a higher temperature is applied, the specimen integrity after failure is low. On the contrary, the specimen integrity is high if a lower temperature is used. As the treatment temperature gradually increases, more fragments can be observed after failure of the specimen.

Figure 9. Failure modes of granite specimens under different treatment temperatures. (**a**) 25 °C (room temperature); (**b**) 400 °C; (**c**) 600 °C; and (**d**) 800 °C.

3.2. Acoustic Emission Characteristic

The AE technique is a method which has been proven to be useful to investigate the microcracking behavior of rock specimens during loading [4,17,37]. As pointed out by Eberhardt et al. [52], the recorded AE activity was mainly associated with grain boundary movement, dislocations, or closure, initiation, propagation, and coalescence of microcracks along or inside mineral grains. In this section, the AE characteristics of the three thermally-damaged rocks are investigated.

The variations of AE parameters in terms of accumulated AE counts and AE hits in response to the change of the axial strain for quartz sandstone specimens under different treatment temperatures are presented in Figure 10. The results show that the evolutions of the two AE parameters can correlate to the stress–strain curves satisfactorily. There is basically no AE signals being detected in the pre-peak deformation stage. The AE signals then initiate and increase rapidly when the stress–strain curve enters into the peak stage, which indicates that the examined quartz sandstone is very brittle. It is also found that as the treatment temperature increases, the AE signals in the initial stage become more prominent, especially for the specimen thermally treated with a temperature of 1000 °C. This is because more microcracks are generated when a higher treatment temperature is applied. The closure of these thermally-induced microcracks will lead to more dramatic AE activities in the initial deformation stage. Meanwhile, as a high treatment temperature is applied, more AE signals will be recorded in the pre-peak stage, indicating that the brittleness of the rock is largely weakened as the treatment temperature increases.

The evolutions of AE parameters in terms of accumulated AE counts and AE hits in the entire deformation process for marble specimens under different treatment temperatures are reported by Rong et al. [17]. It is seen from the results that basically no AE signals are detected in the initial deformation process if the specimen is experienced no thermal damage. The AE signals then begin to increase when the stress is about 0.4 times the peak stress. The AE signals increase rapidly when the stress approaches about 0.8 times the peak strength. However, with an increase of the temperature in the treatment, the AE signals in the initial stage become more prominent. The results indicate that more micro-cracks will be generated as the treatment temperature increases. The total AE signals in the entire deformation process are found to decrease as higher treatment temperature is applied to the specimen.
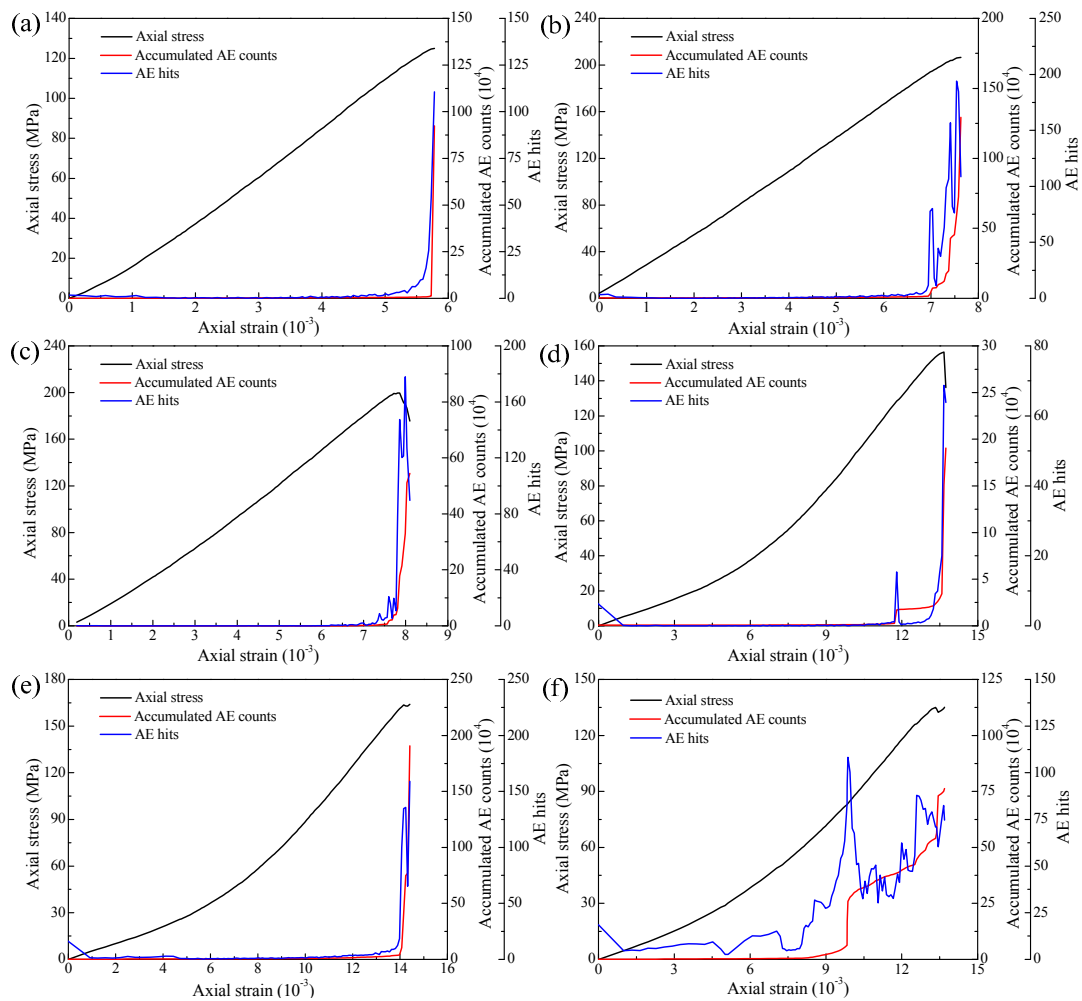
Figure 10. Variations of AE parameters in the deformation process for quartz sandstone specimens under different treatment temperatures. (**a**) 25 °C (room temperature); (**b**) 200 °C; (**c**) 400 °C; (**d**) 600 °C; (**e**) 800 °C; and (**f**) 1000 °C.

Some occasional stress drops in the stress–strain curve can be observed when the treatment temperature is low. The corresponding AE signals recorded at this stage are found to increase drastically. Because the marble specimen is relatively isotropic in texture and the mineral grains are generally well cemented to each other, this "sudden stress drop" phenomenon is mainly associated with the dislocation or breakage of minerals or grain boundary movement in the rock specimen during loading. The sudden slip or breakage of minerals along the grain boundaries will induce a transient stress relaxation, which will result in a sudden stress drop in the stress–strain curve and lead to a large amount of AE activities. However, the "sudden stress drop" phenomenon is not observed when the treatment temperature is high (i.e., 400 °C and 600 °C). The results reveal that the brittleness of the marble specimen is weakened when a higher treatment temperature is applied.

The evolutions of AE parameters in terms of accumulated AE counts and AE hits in the entire deformation process for granite specimens under different treatment temperatures are presented in Figure 11. Similarly to the results of quartz sandstone, almost no AE signals can be detected in the pre-peak deformation stage and the AE signals then multiply when the stress approaches the peak value. The phenomenon exists even when the applied treatment temperature is high. The results indicate that the examined granite is also very brittle. Meanwhile, it is also seen from the results that the total AE signals in the entire deformation process decrease as the applied treatment temperature gradually increases.
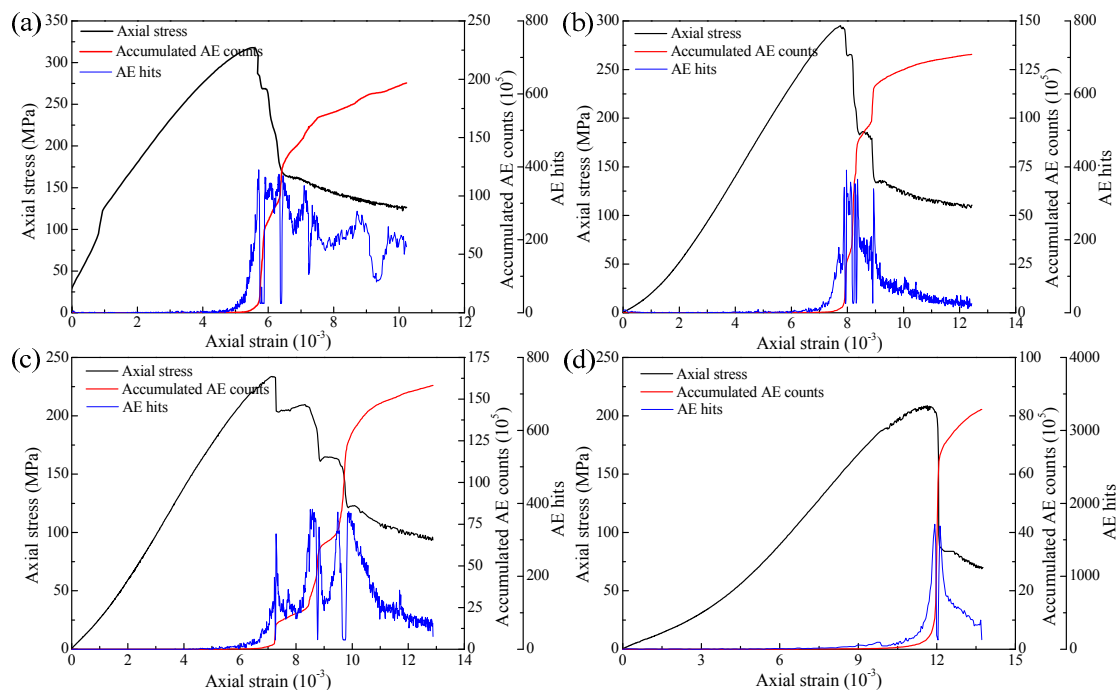
Figure 11. Variations of AE parameters in the deformation process for granite specimens under different treatment temperatures. (**a**) 25 °C (room temperature); (**b**) 400 °C; (**c**) 600 °C; and (**d**) 800 °C.

By comparison of the AE characteristics of the examined three rocks, it is seen that the AE characteristic is different for various rock types. For quartz sandstone and granite, there is seldom AE signals in the pre-peak deformation stage and the AE signals multiply only when the stress approaches the peak stress value. More AE signals can be detected in the pre-peak stage for marble. The results reveal that the quartz sandstone and granite is more brittle than the examined marble, which is comparable with the results obtained from the geological characteristic of the rocks. The failure of quartz sandstone and granite will be violent when the AE energy in the form of microcracking stored in the specimen is high enough. The results are also in a good agreement with the failure modes observed in the quartz sandstone and granite as mentioned in the above section. In addition, because the quartz sandstone and granite is brittle, more AE activities are recorded in the entire loading process when compared with those of marble.

3.3. Discussion

In this study, the influence of high temperature treatment on the mechanical behavior and AE characteristic of three rocks are experimentally investigated. The results show that the mechanical behavior and AE characteristic in response to thermal damage are quite different for the examined three rocks. The mechanical properties, such as P-wave velocity, strength, and Young's modulus of the three rocks generally show a decreasing trend as the applied treatment temperature increases. However, because the quartz sandstone has a large porosity, these mechanical parameters increase to some extent when the treatment temperature is low and show a monotonous decrease as the temperature in the treatment is high. It is indicated that the difference in porosity of rocks has a large influence on the strength and deformation behavior in response to thermal loading. In addition, the results interpreted from stress–strain relation, failure model, and AE characteristic generally reveal that the quartz sandstone and granite are more brittle than the examined marble. Hence, the failure of the two rocks is more violent when compared with that of marble. The results are in a general good agreement with the results obtained from the geological characteristic of the rocks. It is inferred that when a quartz-rich rock is loaded, the failure is more brittle when compared with that of a calcite-rich

rock. This phenomenon is probably due to the fact the quartz has a higher strength and hardness than the calcite.

Overall, the results in this study show that the mechanical behavior and AE characteristic in response to the change of treatment temperature is different for various rock types. Different rocks are associated with different microstructures, including degree of weathering, degree of interlocking, porosity, texture, foliation, mineralogical composition, grain size distribution, and micro-defects such as micro-cracks, voids, and cleavage planes [53–60]. All these factors contributing in influencing the mechanical behavior and AE characteristic of rocks under a post high temperature condition. One limitation of this study is that the microscopic examinations such as X-ray diffraction analysis, microscopic observation using scanning electron microscopy or polarizing microscopy, and X-ray computerized tomography are not conducted. Future work will emphasize on the microscopic investigation of thermal damage effect on rock behavior. These microscopic techniques provides powerful tools in characterizing the thermal cracking mechanism of rocks in response to thermal loading. Anyway, the results in this study provide some insights in understanding the thermal damage on rocks from a microscopic view.

4. Conclusions

This study experimentally investigates the mechanical behavior and AE characteristic of three rocks (i.e., sedimentary, metamorphic, and igneous) after exposure to different high temperatures. The results in this study show that the mechanical behavior and AE characteristics of different rock types in response to thermal treatment are quite different. In general, the mechanical properties including P-wave velocity, compressive strength, and Young's modulus for the three rocks show a decreasing trend as the temperature applied to the rock increases. However, because the examined quartz sandstone has a large porosity, these mechanical properties first increase to a certain extent and then decrease as the treatment temperature increases. In addition, the results interpreted from stress–strain curve, failure mode, and AE characteristic show that the failure of quartz-rich rock (i.e., quartz sandstone and granite) is more brittle when compared with that of calcite-rich rock (i.e., marble). Hence, more AE activities can be detected in quartz sandstone and granite than in marble and the recorded AE activities mostly accumulate when the stress approaches the peak strength. However, the ductility is enhanced to some extent as the treatment temperature increases for the three examined rocks. The accumulated AE activities are also found to show a decreasing trend as the temperature applied to the rock increases.

The results in this study provide some sights in understanding how the differences in rock type (i.e., porosity and mineralogical composition) on the mechanical behavior and AE characteristic of rocks in response to thermal treatment. However, in order to have a more comprehensive examination of how microstructure affects the thermal cracking, microscopic investigation techniques such as X-ray diffraction analysis, microscopic observation using scanning electron microscopy or polarizing microscopy, and X-ray computerized tomography can be used in future studies. This is a promising topic in rock mechanics and rock engineering.

References

1. Ranjith, P.G.; Daniel, R.V.; Chen, B.J.; Perera, M.S.A. Transformation plasticity and the effect of temperature on the mechanical behaviour of Hawkesbury sandstone at atmospheric pressure. *Eng. Geol.* **2012**, *151*, 120–127.
2. Tiskatine, R.; Eddemani, A.; Gourdo, L.; Abnay, B.; Aharoune, A.; Bouirden, L. Experimental evaluation of thermo-mechanical performances of candidate rocks for use in high temperature thermal storage. *Appl. Energy* **2016**, *171*, 243–255. [CrossRef]
3. Yang, S.Q.; Ranjith, P.G.; Jing, H.W.; Tian, W.L.; Ju, Y. An experimental investigation on thermal damage and failure mechanical behavior of granite after exposure to different high temperature treatments. *Geothermics* **2017**, *65*, 180–197. [CrossRef]
4. Rong, G.; Peng, J.; Cai, M.; Yao, M.; Zhou, C.; Sha, S. Experimental investigation of thermal cycling effect on physical and mechanical properties of bedrocks in geothermal fields. *Appl. Therm. Eng.* **2018**, *141*, 174–185. [CrossRef]
5. Gónzalez-Gómez, W.S.; Quintana, P.; May-Pat, A.; Avilés, F.; May-Crespo, J.; Alvarado-Gil, J.J. Thermal effects on the physical properties of limestones from the Yucatan Peninsula. *Int. J. Rock Mech. Min.* **2015**, *75*, 182–189. [CrossRef]
6. Peng, J.; Rong, G.; Cai, M.; Yao, M.D.; Zhou, C.B. Physical and mechanical behaviors of a thermal-damaged coarse marble under uniaxial compression. *Eng. Geol.* **2016**, *200*, 88–93. [CrossRef]
7. Yao, M.; Rong, G.; Zhou, C.; Peng, J. Effects of thermal damage and confining pressure on the mechanical properties of coarse marble. *Rock Mech. Rock. Eng.* **2016**, *49*, 2043–2054. [CrossRef]
8. Li, Z.; Wong, L.N.Y.; Teh, C.I. Low cost colorimetry for assessment of fire damage in rock. *Eng. Geol.* **2017**, *228*, 50–60. [CrossRef]
9. Yavuz, H.; Demirdag, S.; Caran, S. Thermal effect on the physical properties of carbonate rocks. *Int. J. Rock Mech. Min.* **2010**, *47*, 94–103. [CrossRef]
10. Tian, H.; Kempka, T.; Xu, N.X.; Ziegler, M. Physical properties of sandstones after high temperature treatment. *Rock Mech. Rock Eng.* **2012**, *45*, 1113–1117. [CrossRef]
11. Sirdesai, N.N.; Singh, T.N.; Gamage, R.P. Thermal alterations in the poro-mechanical characteristic of an Indian sandstone–a comparative study. *Eng. Geol.* **2017**, *226*, 208–220. [CrossRef]
12. Sirdesai, N.N.; Singh, A.; Sharma, L.K.; Singh, R.; Singh, T.N. Determination of thermal damage in rock specimen using intelligent techniques. *Eng. Geol.* **2018**, *239*, 179–194. [CrossRef]
13. Keshavarz, M.; Pellet, F.L.; Loret, B. Damage and changes in mechanical properties of a gabbro thermally loaded up to 1,000 C. *Pure Appl. Geophys.* **2010**, *167*, 1511–1523. [CrossRef]
14. Chen, Y.L.; Ni, J.; Shao, W.; Azzam, R. Experimental study on the influence of temperature on the mechanical properties of granite under uniaxial compression and fatigue loading. *Int. J. Rock Mech. Min.* **2012**, *56*, 62–66. [CrossRef]
15. Inserra, C.; Biwa, S.; Chen, Y. Influence of thermal damage on linear and nonlinear acoustic properties of granite. *Int. J. Rock Mech. Min.* **2013**, *62*, 96–104. [CrossRef]
16. Rong, G.; Peng, J.; Yao, M.; Jiang, Q.; Wong, L.N.Y. Effects of specimen size and thermal-damage on physical and mechanical behavior of a fine-grained marble. *Eng. Geol.* **2018**, *232*, 46–55. [CrossRef]
17. Rong, G.; Yao, M.; Peng, J.; Sha, S.; Tan, J. Influence of initial thermal cracking on physical and mechanical behaviour of a coarse marble: Insights from uniaxial compression tests with acoustic emission monitoring. *Geophys. J. Int.* **2018**, *214*, 1886–1900.
18. Liang, W.G.; Xu, S.G.; Zhao, Y.S. Experimental study of temperature effects on physical and mechanical characteristics of salt rock. *Rock Mech. Rock. Eng.* **2006**, *39*, 469–482. [CrossRef]
19. Dwivedi, R.D.; Goel, R.K.; Prasad, V.V.R.; Sinha, A. Thermo-mechanical properties of Indian and other granites. *Int. J. Rock Mech. Min. Sci.* **2008**, *45*, 303–315. [CrossRef]
20. Brotóns, V.; Tomás, R.; Ivorra, S.; Alarcón, J.C. Temperature influence on the physical and mechanical properties of a porous rock: San Julian's calcarenite. *Eng. Geol.* **2013**, *167*, 117–127. [CrossRef]
21. Liu, S.; Xu, J. An experimental study on the physico-mechanical properties of two post-high-temperature rocks. *Eng. Geol.* **2015**, *185*, 63–70. [CrossRef]
22. Tian, H.; Kempka, T.; Xu, S.; Ziegler, M. Mechanical properties of sandstones exposed to high temperature. *Rock Mech. Rock Eng.* **2016**, *49*, 321–327. [CrossRef]

23. Mahmutoglu, Y. Mechanical behaviour of cyclically heated fine grained rock. *Rock Mech. Rock Eng.* **1998**, *31*, 169–179. [CrossRef]

24. Liu, S.; Xu, J. Mechanical properties of Qinling biotite granite after high temperature treatment. *Int. J. Rock Mech. Min.* **2014**, *71*, 188–193. [CrossRef]

25. Tian, H.; Ziegler, M.; Kempka, T. Physical and mechanical behavior of claystone exposed to temperatures up to 1000°C. *Int. J. Rock Mech. Min.* **2014**, *70*, 144–153. [CrossRef]

26. Peng, J.; Rong, G.; Cai, M.; Yao, M.D.; Zhou, C.B. Comparison of mechanical properties of undamaged and thermal-damaged coarse marbles under triaxial compression. *Int. J. Rock Mech. Min.* **2016**, *83*, 135–139. [CrossRef]

27. Liu, Q.; Qian, Z.; Wu, Z. Micro/macro physical and mechanical variation of red sandstone subjected to cyclic heating and cooling: An experimental study. *Bull. Eng. Geol. Environ.* **2017**, 1–15. [CrossRef]

28. Yin, T.; Li, X.; Cao, W.; Xia, K. Effects of thermal treatment on tensile strength of Laurentian granite using Brazilian test. *Rock Mech. Rock. Eng.* **2015**, *48*, 2213–2223. [CrossRef]

29. Roy, D.G.; Singh, T.N. Effect of heat treatment and layer orientation on the tensile strength of a crystalline rock under Brazilian test condition. *Rock Mech. Rock. Eng.* **2016**, *49*, 1663–1677.

30. Nasseri, M.H.B.; Schubnel, A.; Young, R. Coupled evolutions of fracture toughness and elastic wave velocities at high crack density in thermally treated Westerly granite. *Int. J. Rock Mech. Min. Sci.* **2007**, *44*, 601–616. [CrossRef]

31. Chaki, S.; Takarli, M.; Agbodjan, W.P. Influence of thermal damage on physical properties of a granite rock: Porosity, permeability and ultrasonic wave evolutions. *Constr. Build. Mater.* **2008**, *22*, 1456–1461. [CrossRef]

32. Yang, S.Q.; Hu, B. Creep and long-term permeability of a red sandstone subjected to cyclic loading after thermal treatments. *Rock Mech. Rock. Eng.* **2018**. [CrossRef]

33. Fan, L.F.; Wu, Z.J.; Wan, Z.; Gao, J.W. Experimental investigation of thermal effects on dynamic behavior of granite. *Appl. Therm. Eng.* **2017**, *125*, 94–103. [CrossRef]

34. Wong, L.N.Y.; Li, Z.; Kang, H.M.; Teh, C.I. Dynamic loading of Carrara marble in a heated state. *Rock Mech. Rock. Eng.* **2017**, *50*, 1487–1505. [CrossRef]

35. Meredith, P.G.; Knight, K.S.; Boon, S.A.; Wood, I.G. The microscopic origin of thermal cracking in rocks: An investigation by simultaneous time-of-flight neutron diffraction and acoustic emission monitoring. *Geophys. Res. Lett.* **2001**, *28*, 2105–2108. [CrossRef]

36. Browning, J.; Meredith, P.; Gudmundsson, A. Cooling-dominated cracking in thermally stressed volcanic rocks. *Geophys. Res. Lett.* **2016**, *43*, 8417–8425. [CrossRef]

37. Griffiths, L.; Lengliné, O.; Heap, M.J.; Baud, P.; Schmittbuhl, J. Thermal cracking in Westerly Granite monitored using direct wave velocity, coda wave interferometry, and acoustic emissions. *J. Geophys. Res.-Solid Earth* **2018**, *123*, 2246–2261. [CrossRef]

38. Chen, Y.; Wang, C.Y. Thermally induced acoustic emission in Westerly granite. *Geophys. Res. Lett.* **1980**, *7*, 1089–1092.

39. Fredrich, J.T.; Wong, T. Micromechanics of thermally induced cracking in three crustal rocks. *J. Geophys. Res.-Solid Earth* **1986**, *91*, 12743–12764. [CrossRef]

40. Freire-Lista, D.M.; Fort, R.; Varas-Muriel, M.J. Thermal stress-induced microcracking in building granite. *Eng. Geol.* **2016**, *206*, 83–93. [CrossRef]

41. Kranz, R.L. Microcracks in rocks: A review. *Tectonophysics* **1983**, *100*, 449–480. [CrossRef]

42. Wang, H.F.; Bonner, B.P.; Carlson, S.R.; Kowallis, B.; Heard, H.C. Thermal stress cracking in granite. *J. Geophys. Res. Solid Earth* **1989**, *94*, 1745–1758. [CrossRef]

43. Zhu, Z.; Tian, H.; Jiang, G.; Cheng, W. Effects of high temperature on the mechanical properties of Chinese marble. *Rock Mech. Rock. Eng.* **2018**, *51*, 1937–1942. [CrossRef]

44. Simmons, G.; Cooper, H.W. Thermal cycling cracks in three igneous rocks. *Int. J. Rock Mech. Min. Geomech. Abstr.* **1978**, *15*, 145–148. [CrossRef]

45. Sprunt, E.S.; Brace, W.F. Direct observation of microcavities in crystalline rocks. *Int. J. Rock Mech. Min.* **1974**, *11*, 139–150. [CrossRef]

46. Homand-Etienne, F.; Houpert, R. Thermally induced microcracking in granites: Characterization and analysis. *Int. J. Rock Mech. Min. Geomech. Abstr.* **1989**, *26*, 125–134. [CrossRef]

47. Zuo, J.P.; Xie, H.P.; Zhou, H.W.; Peng, S.P. SEM in situ investigation on thermal cracking behaviour of Pingdingshan sandstone at elevated temperatures. *Geophys. J. Int.* **2010**, *181*, 593–603.

48. Wang, H.F.; Heard, H.C. Prediction of elastic moduli via crack density in pressurized and thermally stressed rock. *J. Geophys. Res.* **1985**, *90*, 10342–10350. [CrossRef]

49. Clark, S.P. *Handbook of Physical Constants*; Geological Society of America: New York, NY, USA, 1966.

50. Ulusay, R.; Hudson, J.A. The complete ISRM suggested methods for rock characterization, testing and monitoring: 1974-2006. ISRM commission on testing methods. *Environ. Eng. Geosci.* **2007**, *15*, 47–48.

51. Peng, J.; Rong, G.; Cai, M.; Zhou, C.B. A model for characterizing crack closure effect of rocks. *Eng. Geol.* **2015**, *189*, 48–57. [CrossRef]

52. Eberhardt, E.; Stead, D.; Stimpson, B.; Read, R.S. Identifying crack initiation and propagation thresholds in brittle rock. *Can. Geotech. J.* **1998**, *35*, 222–233. [CrossRef]

53. Fredrich, J.T.; Evans, B.; Wong, T.F. Effect of grain size on brittle and semibrittle strength: Implications for micromechanical modelling of failure in compression. *J. Geophys. Res. Solid Earth.* **1990**, *95*, 10907–10920. [CrossRef]

54. Tuğrul, A.; Zarif, I.H. Correlation of mineralogical and textural characteristics with engineering properties of selected granitic rocks from Turkey. *Eng. Geol.* **1999**, *51*, 303–317. [CrossRef]

55. Everitt, R.A.; Lajtai, E.Z. The influence of rock fabric on excavation damage in the Lac du Bonnett granite. *Int. J. Rock Mech. Min.* **2004**, *41*, 1277–1303. [CrossRef]

56. Tuğrul, A. The effect of weathering on pore geometry and compressive strength of selected rock types from Turkey. *Eng. Geol.* **2004**, *75*, 215–227. [CrossRef]

57. Schultz, R.A.; Okubo, C.H.; Fossen, H. Porosity and grain size controls on compaction band formation in Jurassic Navajo Sandstone. *Geophys. Res. Lett.* **2010**, *37*, L22306. [CrossRef]

58. Cheung, C.S.N.; Baud, P.; Wong, T. Effect of grain size distribution on the development of compaction localization in porous sandstone. *Geophys. Res. Lett.* **2012**, *39*, L21302. [CrossRef]

59. Faoro, I.; Vinciguerra, S.; Marone, C.; Elsworth, D.; Schubnel, A. Linking permeability to crack density evolution in thermally stressed rocks under cyclic loading. *Geophys. Res. Lett.* **2013**, *40*, 2590–2595. [CrossRef]

60. Peng, J.; Wong, L.N.Y.; Teh, C.I. Influence of grain size heterogeneity on strength and micro-cracking behavior of crystalline rocks. *J. Geophys. Res. Solid Earth* **2017**, *122*, 1054–1073. [CrossRef]